Australian Journal of Grape and Wine Research

AUSTRALIAN SOCIETY OF VITICULTURE AND OENOLOGY | ASVO

RESEARCH ARTICLE OPEN ACCESS

TiO_2-Coated Glass Spheres as an Advanced Material for Wine Protein Stabilisation

Marina Serantoni[1] | Ilaria Zanoni[1] | Mauro Mazzocchi[1] | Carlo Baldisserri[1] | Giuseppina Paola Parpinello[2] | Andrea Versari[2] | Arianna Ricci[2] | Antoni Szumny[3] | Anna Luisa Costa[1]

[1]CNR-ISSMC Institute of Science, Technology and Sustainability for the Development of Ceramic Materials, National Research Council, Faenza, Italy | [2]Department of Agricultural and Food Sciences, Alma Mater Studiorum, University of Bologna, Cesena, Italy | [3]Department of Food Chemistry and Biocatalysis, Wrocław University of Environmental and Life Sciences, Wrocław, Poland

Correspondence: Ilaria Zanoni (ilaria.zanoni@issmc.cnr.it)

Received: 1 September 2025 | **Revised:** 20 January 2026 | **Accepted:** 23 February 2026

Academic Editor: Paul Kilmartin

Keywords: BSA | glass spheres | protein adsorption | TiO_2 | wine stabilisation

ABSTRACT

Wine protein stabilisation, i.e., the removal of pathogenesis-related proteins (PRPs), is a step in the white wine fining process. Winemakers use bentonite for this purpose. However, its use has drawbacks due to the production of voluminous waste, wine loss during racking, and decrease in wine quality due to the adsorption of colour components and aroma. New materials for stabilising wine proteins are the object of this study. In this context, an engineered production process for TiO_2-coated glass spheres and a use protocol were developed as an alternative to bentonite treatment, providing relevant information for process scalability. This paper describes the wine protein adsorption capability of a patent-based, innovative material consisting of thin layers of TiO_2 nanoparticles supported on food-grade glass spheres, to be used for the protein stabilisation of wine in a flow process. Protein removal was assessed by the heat test and Pierce's test on unstable wines. As a safety-related criterion, the amount of TiO_2 released during use was quantified by ICP–OES. The possibility of regenerating the material during use and recycling it at the end of life was also investigated, together with a preliminary cost assessment. Overall, the proposed solution follows a "safe and sustainable by design" (SSbD) approach, matching functionality (selectivity for proteins and heavy metals), safety, cost and recyclability criteria.

Highlights

1. TiO_2-coated glass spheres were successfully tested for wine protein stabilisation.
2. The wine-treatment process was engineered, providing insights for scale-up.
3. Protein removal was verified by the heat test protocol and Pierce's test.
4. TiO_2 release during use was quantified by ICP–OES ($< 0.5\ mg\ L^{-1}$).
5. Material regeneration, reuse and end-of-life recycling were experimentally evaluated.

1 | Introduction

In the wine market, the formation of haze in bottled wine can generate concern among consumers who prefer to buy clear and transparent wine. Haze formation can occur due to protein instability and coagulation at elevated temperatures that can arise during the shipping or storage of bottled wine. The unstable proteins are pathogenesis-related proteins (PRPs), mainly thaumatin-like and chitinase proteins, with molecular weights between 10 and 40 kDa and an isoelectric point below six [1–6]. Bentonite is still the most efficient fining agent in achieving protein stability in white wines, although its use is deemed to have a significant effect on wine quality [7, 8]. The study of innovative materials as substitutes for bentonite in wine fining is

a current area of interest, driven by scientific challenges and economic considerations [9–15]. In agreement with the "safe and sustainable by design" (SSbD) framework launched by the European Commission [16] and already applied in many European projects, the innovative materials should satisfy safety and sustainability criteria across their life cycle, by ensuring controlled worker exposure during the production stage, avoiding the use of the potentially hazardous substance and promoting recyclability or new use of material, at the end of the life. TiO_2 as nanopowder is known for its protein affinity [17–19], and it was tested for wine protein adsorption in the laboratory [20, 21]. Even if the tests were very promising [22], it became clear that the nanopowder could not be used to treat wine due to its difficulty in separating it from wine after protein adsorption. It is necessary to engineer the TiO_2 nanopowder as a thin layer supported by an inert material. TiO_2 thin layers' engineering has been the subject of many studies because they have applications in catalysis and water waste treatment [23–26]. The thin layer adhered to supporting materials can be prepared by physisorption and immobilisation of the particles by spray or dip-coating [27, 28], by the precursor's deposition and in situ nucleation [29], by aerosol-assisted chemical vapour deposition [30]. To develop a reliable and effective strategy for wine protein adsorption, the TiO_2 layer must show high adhesion to the surface of the inert support and the adsorption capability of the TiO_2 nanomaterial should remain unaltered, as well as its surface reactivity and high specific surface area. Additionally, the proposed material should be cost-effective and able to compete with bentonite in the market. The authors have previously demonstrated the suitability of a composite TiO_2–glass substrate [31], then combined with a continuous flow process, for protein stabilisation in white wines [32]. In this study, the proposed technology was further validated by depositing a TiO_2 nanopowder paste onto glass spheres at lab-batch scale and comparing the results with those obtained using the more commonly employed nanosol-based deposition method. We evaluated the capacity of TiO_2-coated glass spheres to absorb protein by using a model wine solution containing bovine serum albumin (BSA, 66 kDa). BSA was used as a model reference protein. Although BSA (66.5 kDa) has a higher molecular weight than wine PR proteins (10–40 kDa), it was selected based on its comparable surface charge under wine pH conditions [4, 33–35]. Its larger size represents a conservative experimental condition for evaluating adsorption performance. We tested the possibility of regenerating several times the materials by a mild basic water treatment after BSA absorption from the model wine solution. The most effective TiO_2-coated material was tested with a rosé wine requiring 1 g/L of bentonite to be stabilised using the conventional treatment, as reported by the provider. Then, a scale-up and regeneration test was performed using 1 kg of TiO_2 paste-coated spheres and 3 L of target wine (unstable Pinot blanc). We assessed the cost of the proposed technology compared to bentonite, considering the advantages of the regeneration process. The whole design asset allowed us to demonstrate the quality of this innovative material for food-grade applications.

2 | Materials and Methods

2.1 | Glass Sphere Surface Treatments

The inert supports for the adsorbing material were 5-mm-diameter food-grade glass spheres (Preciosa Ornela, a.s., Desná, Czech Republic), Table S1. The spheres were sandblasted in the laboratory to improve the adhesion of the thin layers. For the nanosol case, a basic (TB) or acidic treatment (TA) was applied to the glass surface to activate the glass surface sites. A 6 M NaOH solution was used for the TB of glass sandblasted spheres, whereas glacial acetic acid (PubChem 176, Sigma-Aldrich) was used for the TA. Spheres were soaked in the acidic or basic solutions for 20 h and then washed with deionised water until a neutral pH was reached.

2.2 | TiO_2 Nanosol Thin-Layer Coatings

To obtain TiO_2 nanosol coating, the acidic or basic-treated sandblasted spheres were soaked for 1 h in TiO_2 or TiO_2@SiO_2 nanosol solutions. The TiO_2 nanosol (2% w/w) solution was a commercial nanodispersion of TiO_2 (TiO_2 anatase, 6% w/w; nanoparticle size 40 nm, polydispersity index 0.25, pH 5, PARNASOS PH000025 Colorobbia Consulting S.r.l. Italia). The TiO_2@SiO_2 nanosol was prepared by adding a 6% w/w SiO_2 suspension (LUDOX Colloidal Silica) to the 2% w/w TiO_2 suspension. The TiO_2@SiO_2 nanosol was mixed for 48 h to obtain a 1:3 stable suspension. The entire coating procedure was reported in previous work [36]. The treated spheres were then dried in an oven at 70°C for 45 min and fired at 400°C for 3 h to obtain a sintered thin layer of nanoparticles adhered to the inert glass surface.

2.3 | Paste-Based TiO_2 Thin-Layer Coating

A paste made of TiO_2 Aeroxide P25 Degussa (PubChem ID 26042) was prepared by mixing the nanopowder with ethanol (PubChem ID 702), terpineol (PubChem ID 17100) and ethyl cellulose (PubChem ID 24832091) as reported in Patent No. 102018000004721 [32]. From the SSbD perspective, this is the only step in the preparation process of the TiO_2 paste-coated sphere in which the TiO_2 is handled in the nanopowder form. The paste was applied to the glass spheres (only sandblasted) and fired at about 500°C.

2.4 | TiO_2-Coated Sphere Washing Pretreatment

After firing, the TiO_2-coated spheres underwent water washing cycles to remove loosely bound agglomerates of TiO_2 nanoparticles. Turbidimetry and ICP–OES analysis on the washing water were conducted to estimate the TiO_2 release. After washing, the spheres were dried by an air flux and made ready for the protein adsorption tests. For the TiO_2 nanosol-coated spheres, a 15-g sample of spheres was left in contact with 25 mL of water for 10 min, and then, the water was analysed by turbidimetry and ICP–OES, and the procedure was repeated three times. For the TiO_2 paste-coating spheres, 900 g of spheres was inserted inside a separating funnel and added with 450 mL of water for each wash. To avoid occlusion of the separating funnel, a home-made Teflon separating septum was placed at the bottom of the funnel cone. The water was left in contact with the sphere in the separating funnel for 25 min each time and then drawn from the tap, and the procedure was repeated nine times.

2.5 | Wine Solutions

A model wine solution was prepared by adding to deionised water (Milli-Q, 18.5 MΩ cm), in sequence: ethylic alcohol 13% w/w (PubChem ID 702), tartaric acid 5 g/L (PubChem CID 875)

and NaOH 5 M (PubChem CID 14798) to bring the model wine solution to pH 3.5. BSA (PubChem CID 6432) was added to the model wine solution as a reference protein. Na_2SO_4 (PubChem CID 24436) was used to promote the coagulation and precipitation of the BSA at high temperatures (HTP–BSA method). All chemicals were purchased by Sigma-Aldrich and used as received. Rosé wine (vintage 2021) was provided by DLR Rheinpfalz, DE, Table S2. White wine, Pinot blanc (vintage 2022), was provided by DISTAL, University of Bologna.

2.6 | Z-Potential Measurement

The zeta potential of TiO_2 nanoparticles or BSA in model wine solution was determined by electrophoretic light scattering measurements, using a Zetasizer Nano ZSP (model ZEN5600, Malvern Instruments, UK). Samples were measured three times, and data were obtained by averaging the three measurements. Z-potential (Z_p) measurement versus pH curves was recorded using the instrument coupled with an automatic titrating system, evaluating the superficial charge from ca. 2.5–4.5 pH units. We performed several zeta potential measurements using model wine solutions (pH 3.5) of nanosols, nanopowder and BSA molecules: TiO_2 (Colorobbia nanosol), TiO_2@SiO_2 (from CNR synthesis), SiO_2 (Ludox nanosol), TiO_2 Aeroxide P25 Degussa and BSA.

2.7 | Field-Emission Scanning Electron Microscope (FE-SEM) Analysis

The surface structural features of TiO_2-coated spheres were observed by scanning electron microscopy analysis using a Carl Zeiss Sigma NTS (Gmbh Oberkochen, Germany) field-emission scanning electron microscope (FE-SEM), after coating the sphere with a 5-nm layer of gold.

2.8 | Elemental Analysis, ICP–OES

To detect the concentration of TiO_2 released in washing water, model or real wine, and to estimate the variation in the concentration of other ions in wine due to spheres' treatment, we measured the Ti, Cu and Fe content by ICP–OES analysis (ICP–OES 5100—vertical dual-view apparatus, Agilent Technologies, Santa Clara, CA, USA). We used the following wavelengths: Ti at 335 nm, Cu at 327 nm and Fe at 260 nm. To detect the concentration of BSA, we measured the concentration of sulphur in the wine solution model, using the calibration curve reported in Figure S6b (sulphur wavelength at 183 nm). All calibration curves had a correlation coefficient limit higher than 0.999. The calibration fit was linear, including a blank in calibration. Argon was selected as the internal standard (wavelength 420 nm). The precision of the measurements expressed as RSD% for the analysis was always less than 5%. The limit of detection (LOD) at the operative wavelength for Ti, Cu and Fe was 0.01 mg/L. Before model wine analysis, samples were diluted 1:8 with ultrapure water to decrease the alcoholic content. All samples were acid-digested by adding a 10% volume of nitric acid (HNO_3 65%).

2.9 | UV/Vis Analysis

To detect the concentration of BSA by UV/Vis spectroscopy (UV/Vis/NIR Spectrometer Lambda 750, PerkinElmer), the BSA content was evaluated by the intensity of the adsorption peak at $\lambda = 280$ nm [37]. The calibration curve was obtained by plotting known BSA concentrations as a function of the relative absorbance value (Figure S6c, blue dots). The calibration curve showed correlation coefficients (R^2) above 0.99. UV/Vis spectroscopy results were the average of three independent measurements.

2.10 | Heat Test Protocol

All turbidimetry measurements were performed by a TURBIDIMETER AQUALYTIC AL 255T-IR (EN ISO 7027). The instrument measures the turbidity of a solution as a nephelometric turbidity unit (NTU) in a range of 0.01–1100, with a detection limit of 0.01 NTU, using an 860 nm LED. The heat test [38] measures the turbidity caused by the artificial coagulation at high temperatures of low-weight wine proteins, which is proportional to the protein content. This test simulates what could naturally happen to wine if it undergoes a rise in temperature during transport or storage [39, 40]. The heat test procedure used in this work consisted of keeping the wine for 30 min at 80°C, cooling it for 45 min at room temperature, and immediately measuring the turbidity. The NTU measurement values have an associated error of ± 0.05 NTU. A wine is considered stable if the difference in turbidity, before and after the heating treatment (Δ NTU = NTU2 − NTU1), does not exceed the value of 2 NTU [41].

2.11 | HTP–BSA

In this study, the heat test protocol was applied to evaluate the adsorption capability of the innovative material using a model wine solution containing BSA. This procedure will be referred to as the HTP–BSA method throughout this paper. A calibration curve was built using solutions of known BSA concentration and measuring the NTU values after heating (NTU2, heat test). Because BSA is a very stable protein [42], even at elevated temperatures, to force its coagulation during the heat test, the principle of the salting-out method [43, 44] was applied. A known amount of salt (Na_2SO_4, PubChem CID 24436) was added to the model wine solution to facilitate the BSA coagulation. The correct amount of salt to be added (0.015 M) was experimentally determined. To test the adsorption capability of the TiO_2-coated spheres, a model wine solution of known BSA content (140 mg/L) was added to the TiO_2-coated spheres in a separating funnel (volume ratio 1:2, respectively) and left in contact for 1 h. The solution was then drawn from the tap of the separating funnel. Na_2SO_4 was added, heated and cooled, and its NTU2 turbidity value was measured, following the heat test protocol. The NTU2 value was inserted in the calibration curve to infer the BSA content after contact with the spheres. The difference between the BSA content of the solution before and after the spheres' contact indicated the BSA adsorption capability of the TiO_2 material.

2.12 | Pierce's Test

Pierce's test measured the concentration of proteins in the wine samples before and after sphere treatment. This test is based on a bicinchoninic acid (BCA) protein method (code BCA1-1KT, Sigma-Aldrich, Milan, Italy), which relies on the reduction of Cu^{2+} to Cu^{1+} by proteins under alkaline conditions, followed by the formation of a BCA–copper complex. The resulting complex was quantified by UV/Vis absorbance at 562 nm. Protein

concentration was determined from colorimetric data using an experimental calibration curve, as described in reference [45].

2.13 | TiO_2-Coated Sphere Regeneration

To regenerate the TiO_2-coated spheres after protein adsorption, the spheres were soaked in a 0.5 M NaOH (PubChem CID 14798) solution for 1 h, rinsed with deionised water until a neutral pH was reached (Figure S1) [46] and then dried by compressed air flux. The spheres were kept inside the separating funnel during all steps.

2.14 | Wine Treatment Protocol

For each sphere treatment cycle, 500 g of TiO_2-coated spheres was loaded into a laboratory-scale cartridge: a separating funnel. Subsequently, 250–300 mL of wine was introduced into the separating funnel and kept in contact with the spheres for 1 h at room temperature in the dark. After the contact time, the treated wine was recovered by gravity-driven drainage from the funnel pipe, completing one stabilisation cycle. This laboratory procedure was intentionally designed to simulate a cartridge-based flow treatment system, in which wine passes through a packed bed of functionalised spheres under controlled residence time. Following each treatment, the spheres were regenerated as described above, enabling multiple reuse cycles. Although performed at laboratory scale, the experimental setup was engineered to reproduce the key operational features of a continuous flow system, including contact time, solid/liquid ratio and regeneration protocol, thus providing directly transferable information for future scale-up.

3 | Results and Discussion

3.1 | Zeta Potential Measurement in Model Wine Solution

We carried out a series of zeta potential measurements to investigate the interactions between TiO_2-based nanoparticles, constituting the coating of the nanospheres, and BSA, chosen as the target protein in a model wine solution. It is known from the literature [47] that the TiO_2 Colorobbia nanosol dispersed in water has the isoelectric point, IEP_{H2O} at pH = 7, while the IEP_{H2O} of BSA in water is at pH = 3.7. For TiO_2 P25 Degussa, the IEP_{H2O} in water is at pH = 6. Nevertheless, Figure 1 shows that in the model wine solution, the TiO_2 Colorobbia nanosol and TiO_2 P25 Degussa are negatively charged ($Z_p \sim -25$ mV), while the BSA molecules are positively charged ($Z_p \sim +12$ mV), in the pH range investigated (pH 2.8–4.3). SiO_2 and TiO_2@SiO_2 samples showed, as well, a negative Z_p, even if lower than TiO_2 (Z_p from 0 to −5 mV). We suppose that the high concentration of tartaric acid in the model wine solution promotes the specific adsorption of negatively charged molecules onto the TiO_2 surface, causing the IEP to shift towards an acidic pH. In addition, as reported in the literature [48], the electrical double layer of corrugated interfaces can trigger changes in the electrostatic potential due to double-layer self-overlap and regulation effects inside porous. An enhancement of the adsorption of negative anions inside the porous material could induce a further shift towards a lower pH of the TiO_2 isoelectric point. The greater charge difference between BSA and TiO_2, compared to SiO_2, accounts for the higher BSA adsorption. In addition, the strong electrostatic attraction between oppositely charged surfaces could explain the selectivity of the TiO_2-coated spheres, which preferentially attract positively charged molecules, thereby limiting the adsorption of negatively charged compounds such as polyphenols.

3.2 | Surface Structural Features of TiO_2 Nanosol-Coated Spheres

To find the best condition to maximise the adhesion of the nanoparticles thin-layer to the glass support, the sandblasted glass surface was pretreated with acidic (TA), basic solution (TB) or left untreated (TQ). Six samples of spheres were then prepared as shown in Table S3.

Figure S2 shows FE-SEM images of the (a) "as received" and (b) sandblasted surface of spheres, highlighting how the sandblast sphere treatment increased the surface roughness of the glass spheres. Figure S3 shows the surface of TiO_2 nanosol-coated spheres: It is possible to see that, for the (a) TQ–TiO_2 and (e) TB–TiO_2 samples, the surface of the sphere is covered by a layer that can be estimated, from the fractures visible in the FE-SEM images, as having a thickness from 1 to 2 microns; for (c) TA–TiO_2 and (b) (d) (f) TiO_2@SiO_2-coated spheres, the layer appears very thin and compact with some agglomerations of micrometric particles randomly distributed on the surface. The micrometric aggregates appear poorly adhered to the surface, and therefore, they could be easily detached from it when in contact with aqueous solutions.

3.3 | Surface Structural Features of TiO_2 Paste-Coated Spheres

FE-SEM images reported in Figures 2(a) and 2(b) show the TiO_2 paste-coated glass sphere surface. The TiO_2 layer coating was generally homogeneous. From the layer discontinuity observed in Figure 2(a), it was possible to estimate the TiO_2 layer as having a thickness lower than 1 μm. Figure 1(b) shows a magnification of the TiO_2 thin layer formed by partially sintered nanoparticles of about 30 nm diameter, with pores of dimensions from 50 to 150 nm. Considering the dimension of the BSA of about 7- to 10-nm radius, we suppose that this protein or others with the same size can be easily trapped inside the nanoporous structure or be adsorbed onto the TiO_2 surface (−OH groups) [49, 50].

3.4 | TiO_2-Coated Spheres Washing Pretreatment Results

To avoid turbidity and undesired contamination, we performed several washing cycles of the coated spheres to eliminate TiO_2 aggregates not adhered to the surface. Figures S4 and S5 and Figure 3 report the results of the analysis on the washing water (turbidimetry and ICP–OES) for the TiO_2 nanosol-coated and TiO_2 paste-coated spheres, respectively. For the TiO_2 nanosol coating, the turbidity remained constant after the second washing cycle and in the range of 0.5–1.5 NTU, suggesting a continuous, even if low, release of nanoparticles ($TiO_2 <$ 0.04 mg/L; i.e., Ti < 0.024 mg/L, see Figure S5). No significant difference was observed despite the sphere's acid or basic pretreatments or comparing TiO_2 or TiO_2@SiO_2 nanosols. The TiO_2 release from the TiO_2 paste-coated spheres started with an initial value of 0.3 mg/L and decreased to a very low value after the fifth cycle (Figure 3). After the seventh cycle, it was not possible to

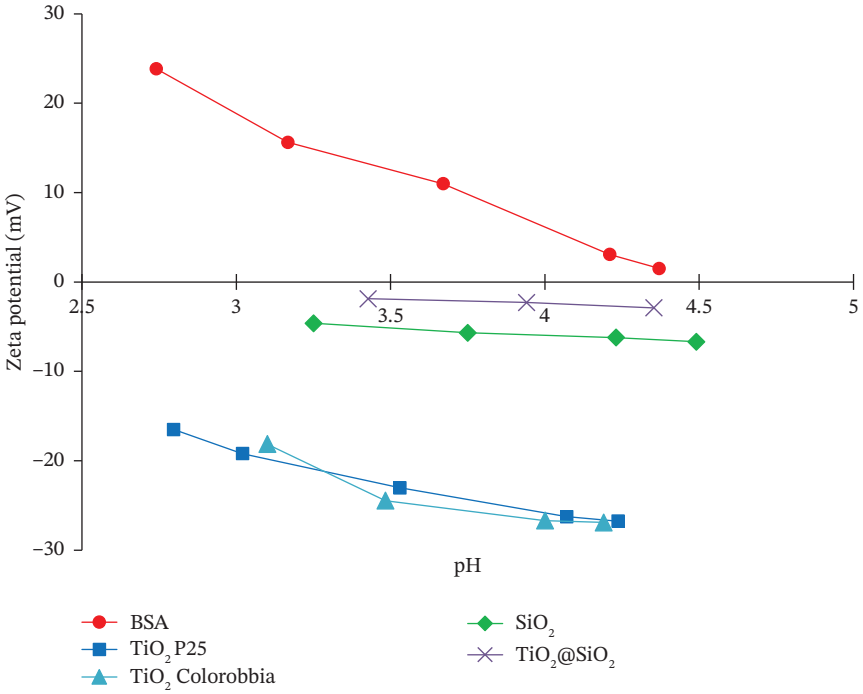

FIGURE 1 | Zeta potential values of BSA molecules, TiO_2 P25, TiO_2 Colorobbia nanosol, SiO_2 ludox nanosol, $TiO_2@SiO_2$ nanosol in model wine solution.

detect the TiO_2 presence, both by turbidity measurements and ICP analysis.

3.5 | BSA Adsorption in Model Wine Solution

We employed three techniques to measure the adsorbed BSA on the TiO_2-coated spheres: HTP–BSA, ICP–OES and UV/Vis analysis (see ESI, BSA Paragraph; Figures S6a–c, and S7). Table 1 reports the percentage of BSA adsorbed, as determined by the turbidimetry calibration curve. The TiO_2 nanosol-coated spheres adsorbed an average of 25% of the BSA, Figure S6a (yellow dots), TQ–TiO_2 reached 27%, while only an average of 11% of BSA was adsorbed by the $TiO_2@SiO_2$ nanosol-coated spheres (Figure S6a, red dots). These results suggested that the TiO_2 nanosol-coated surface was more effective in adsorbing the BSA than the $TiO_2@SiO_2$ nanosol-coated surface. For the TiO_2 paste-coated spheres, the analysis results indicated that around 35% of the BSA was adsorbed, as shown in Figure S6a (green dot). This analysis

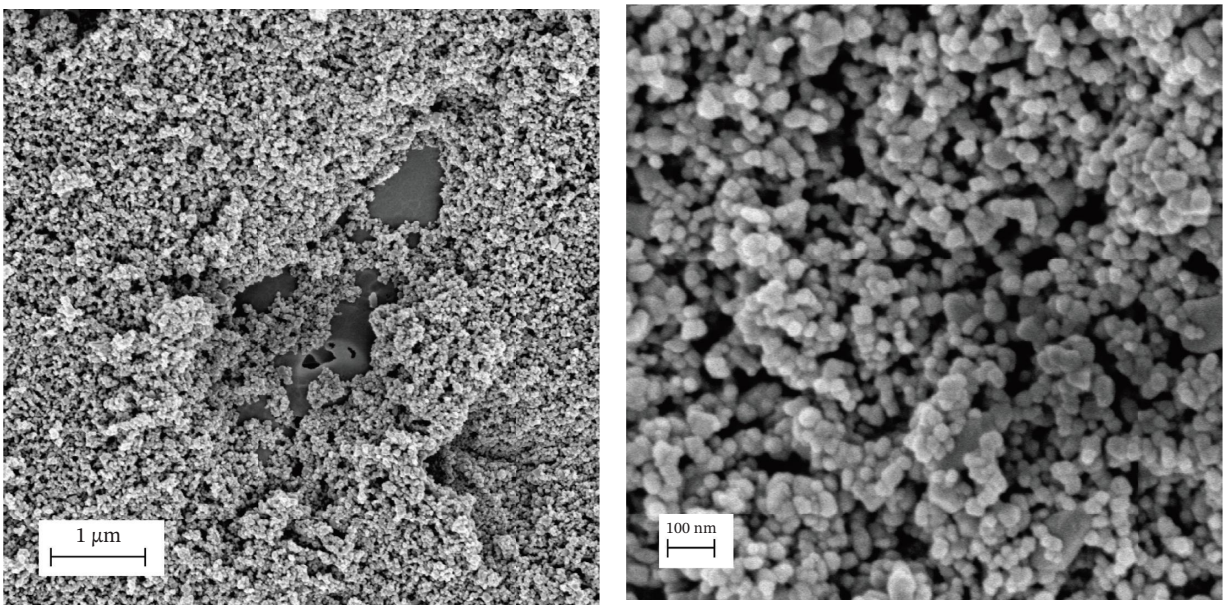

(a) (b)

FIGURE 2 | (a) and (b) FE-SEM images of the TiO_2-coated layer surface. Layer discontinuity shown in Figure 1(a) allowed us to estimate the TiO_2 layer as having a thickness < 1 micron.

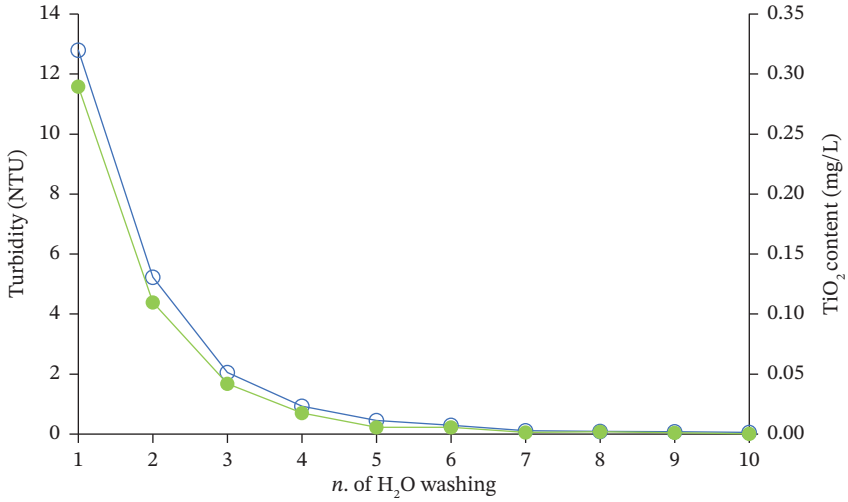

FIGURE 3 | TiO_2 release from TiO_2 paste-coated spheres during washing cycles: turbidity (NTU values, blue line) and TiO_2 release (elemental analysis, green line).

showed that the TiO_2 paste-coated material has the highest ability to adsorb a model protein from the model wine solution and the HTP–BSA method resulted in a more sensitive, direct and cheap method with respect to ICP–OES and UV/Vis analysis, to measure the BSA content in the model wine solution.

Because of these results, the TiO_2 paste-coated spheres material was considered the most promising for testing with wine solutions.

3.6 | Regeneration Test of TiO_2 Paste-Coated Spheres

We performed a material regeneration test using a model wine solution to assess whether the material could be reused multiple times after protein adsorption and regeneration. The amount of BSA adsorbed during successive treatment cycles decreased from an initial value of ca. 38% to a final value of ca. 28% (Figure S8a). The normalised adsorption percentage stabilised at around 75% in the fourth cycle and remained at this level up to the eighth cycle (Figure S8b), confirming the material's ability to be reused for at least eight cycles. To further validate the proposed technology, we assessed the potential release of TiO_2 during the use phase, measuring after each cycle, the content of Ti by ICP–OES analysis (Figure S9) in the model wine solution. The results showed that TiO_2 release decreased from about 0.5 mg/L (Ti = 0.3 mg/L) in the first cycle, to about 0.01 mg/L (Ti = 0.005 mg/L) in the seventh cycle, to an undetectable level at the eighth cycle, always remaining below the food safety values.

TABLE 1 | NTU2 turbidity data, BSA concentrations and adsorbed BSA percentage from the model wine solution after contact with the coated spheres; the error in the NTU values is estimated as ±0.05 NTU.

	NTU2	BSA (mg/L)	BSA adsorbed (%)
TA–TiO_2@SiO_2	61.45	133	5
TQ–TiO_2@SiO_2	59.52	129	8
TB–TiO_2@SiO_2	55.79	121	13
TB–TiO_2	49.22	107	24
TA–TiO_2	48.76	106	24
TQ–TiO_2	47.09	102	27
TiO_2 paste	42.00	91	35

Note: Starting concentration of BSA 140 mg/L.

3.7 | Rosé Wine Stabilisation Treatment

The TiO_2 paste-coated spheres were tested with unstable Rosé for protein adsorption. Figure 4 shows the setup used for a treatment cycle. The heat test results of the treated rosé gave a ΔNTU = 1.8, lower than 2, indicating that the stabilisation was achieved. To confirm the stabilisation due to protein adsorption, we measured the amount of protein by Pierce's test before and after the treatment. The results showed that the protein content in the untreated rosé wine was 920 mg/L, while the treated wine had a protein level of 820 mg/L, reflecting an 11% protein content reduction due to the sphere treatment. The percentage of protein adsorbed is most likely referred to small-size proteins (20–40 kDa), responsible for wine instability, with dimensions compatible with the nanostructured TiO_2 paste-coating (pore's dimension 50–100 nm).

We also measured the adsorption capability of TiO_2 paste-coated spheres for copper and iron ions, as well as the release of TiO_2. ICP–OES results on treated rosé wine showed that copper and iron ions' concentrations decreased after the treatment, as shown in Table S4. This made the wine less oxidisable, reducing the probability of the oxidation process that leads to hydrogen peroxide formation [8].

3.8 | TiO_2 Release During the Use of TiO_2 Paste-Coated Spheres

To address potential safety concerns due to the release of TiO_2 during wine stabilisation, the TiO_2 content was quantified by ICP–OES before and after treatment in rosé wine. As reported in Table S4, the TiO_2 concentration of 0.5 mg/L (equivalent to Ti = 0.3 mg/L) is lower than the limit established by German rules [51] of Ti = 1 mg/L. Moreover, as shown for the test with the model wine solution (Section 3.6), TiO_2 release progressively decreased upon successive reuse cycles, reaching values close to the instrument detection limit.

FIGURE 4 | Rosé wine in the separating funnel in contact with the TiO_2 paste-coated glass spheres.

Concerning the safety of TiO_2 in food and beverages, the European Food Safety Authority (EFSA) 2021 re-evaluation [52] concluded that titanium dioxide (E171) can no longer be considered safe as a 'food additive' due to unresolved genotoxicity concerns and the impossibility of establishing a health-based guidance value. However, the same report states that a dosage below 1 mg/kg body weight per day of TiO_2 micropowder (E171) or 100 mg/kg of nanostructured TiO_2 (< 30 nm) does not cause adverse effects. In this application, TiO_2 is not intentionally added to wine, but detected exclusively as a result of unintentional release from the coated spheres. Therefore, this application should be regarded as a food-contact use rather than as a food additive.

Given the uncertainties highlighted by EFSA, a precautionary approach was adopted in this study. Accordingly, exposure was minimised at source by engineering a strongly immobilised coating and by controlling operating conditions. TiO_2 release was experimentally quantified and remained below 0.5 mg/L under all tested conditions. Referring to these limit values, we can conclude that the Ti/TiO_2 concentrations measured in this study are well below a threshold considered acceptable to ensure food safety.

3.9 | Scale-Up for the Stabilisation of White Wine

After the positive results obtained with the rosé wine, 1 kg of TiO_2 paste-coated spheres was used to stabilise 3 litres of unstable white wine (Pinot blanc, 11.5% alcohol strength, pH 3.1, 225 mg/L total polyphenols). To treat 3 L of wine, two separate separating funnels were used, each filled with 500 g of TiO_2-coated spheres and 300 mL of unstable wine. The spheres were regenerated nine times, allowing all the wine to be treated twice. The unstable white wine exhibited an initial ΔNTU of 25.87, which decreased to 11.15 after filtration using a 0.45-μm membrane filter. Subsequently, the wine underwent an initial sphere treatment, which reduced the ΔNTU to 6.5. A second sphere treatment was required to further decrease the ΔNTU, ultimately reaching a value of 1.64, confirming that the wine had achieved a stable condition. Overall, the same batches of spheres were reused, with nine regeneration steps, keeping their adsorption ability over 80%.

3.10 | Recyclability of TiO_2-Coated Sphere

To test the recyclability of the materials, we detached the TiO_2 from the surface of the glass spheres by ultrasonication in water. The cleaned glass spheres have been successfully reused, and, in principle, the TiO_2 water solution coming from the ultrasonication treatment could be employed for other uses, for example, to prepare TiO_2 aqueous solutions for paint [53].

3.11 | Cost Assessment

The TiO_2 paste-coated spheres are produced using commercially available materials and standard processing steps. An important advantage of the proposed system is the possibility of using the spheres in a flow-through system (cartridge), both during the wine treatment and during the regeneration cycles, which can be performed using reagents commonly employed in the wine industry (diluted caustic soda solutions), thus involving low operational and environmental impact. In addition, the material can be recycled at the end of its life, reducing waste generation. By contrast, bentonite disposal after treatment must be managed by wineries as special waste, involving additional operational costs and environmental burdens. Furthermore, bentonite fining typically results in 3%–10% wine loss, which negatively affects

process efficiency and overall sustainability. It is also well documented that winery practices often lead to an overestimation of bentonite dosage relative to actual protein content, further increasing costs and waste generation. The integration of TiO_2-coated spheres into a flow-through system enables precise control of process parameters and allows protein stabilisation to be achieved within a few hours (Patent No. 102018000004721 [32]).

This represents a significant reduction in processing time compared to conventional bentonite fining, which usually requires 2–4 days. A preliminary and laboratory-scale cost estimation for the preparation and use of TiO_2 paste-coated spheres yielded a value of 0.35 €/L^{-1}, while industrial bentonite treatment costs range between 0.0056 and 0.039 €/L^{-1} (Progetto Vinosme, University of Padova, Italy) [54]. It is important to underline that this estimation should be regarded as indicative only, since it does not account for several factors that are expected to substantially impact the economics at industrial scale, including process scale-up, repeated material regeneration and reuse, reduced labour and energy costs due to shorter processing times, elimination of waste disposal costs and potential value recovery from recycled materials.

Therefore, while the current laboratory cost of the TiO_2-coated spheres-based system is higher than that of bentonite, the technical feasibility and circular use potential of the proposed material support its further development and optimisation. Future work will focus on cost reduction strategies, including increasing TiO_2 loading efficiency and improving the surface-to-volume ratio of the support material.

4 | Conclusions

This study investigates the capability of TiO_2 nanoparticles thin layers supported on food-grade glass spheres for wine protein stabilisation, exploiting their protein adsorption capacity as a potential alternative to bentonite in wine fining processes. BSA adsorption measurements in a model wine solution revealed an enhanced adsorption capacity for the TiO_2 paste-coated glass spheres (about 35%) compared to those coated with TiO_2 nanosol (about 27%). Based on these adsorption results and the absence of detectable TiO_2 release after seven water washing cycles, the TiO_2 paste-coated material was selected for subsequent testing with real wine. To assess the potential for reducing material costs by reusing it multiple times, a regeneration test was conducted using the model wine solution for the TiO_2 paste-coated spheres. The BSA adsorption capacity decreased over the first four cycles, subsequently stabilising, with an overall reduction from an initial 38%–28% by the eighth cycle. ICP–OES analysis revealed TiO_2 release levels below the EU regulatory limit for titanium (Ti < 1 mg/L), decreasing from 0.5 mg/L after the first cycle to 0.01 mg/L after the seventh cycle. Based on these results, the TiO_2 paste-coated material was selected for subsequent testing with real wine. The TiO_2 paste-coated spheres were preliminarily tested for protein adsorption with unstable Rosé wine, and then, a successful scale-up test was performed, using 3 L of unstable Pinot blanc and 1 kg of TiO_2 paste-coated spheres. For the scale-up test with Pinot blanc, the spheres were regenerated nine times, allowing all the wine to be treated twice. Overall, this study successfully demonstrated that the immobilised TiO_2 adsorbing material can serve as a viable alternative to bentonite in wine fining, addressing key limitations such as prolonged processing times for sedimentation and racking, as well as the high costs associated with waste disposal. From the SSbD perspective, the low release of TiO_2 during use, combined with the material's regeneration and recyclability properties, aligns with SSbD criteria and circular economy principles.

Acknowledgements

We thank Antonio Crimaldi for the UV/Vis analysis and Claudio Capiani for the spheres' sandblasting (CNR-ISSMC). We thank Prof. Dr. U. Fischer (DLR Rheinpfalz, DE) for the Rosé wine procurement.

This work was supported by ERA-NETs SUSFOOD2 and CORE Organic Cofunds Joint Call 2019 "Towards sustainable and organic food systems," Mild Innovative Treatment for Wine Stabilisation, "MI WINE" Id.87.

Funding

This study was funded by ERA-NETs SUSFOOD2 and CORE Organic Cofunds Joint Call 2019 "Towards sustainable and organic food systems," Mild Innovative Treatment for Wine Stabilisation, "MI WINE" Id.87. Open access publishing was facilitated by Consiglio Nazionale delle Ricerche, as part of the Wiley-CRUI-CARE agreement.

Conflicts of Interest

Giuseppina Paola Parpinello, Andrea Versari, Arianna Ricci, and Marina Serantoni are co-authors of the Patent No. 102018000004721, Giuseppina Paola Parpinello, Andrea Versari, L. Ragni, Arianna Ricci, Marina Serantoni, and A. Balducci," Device for the stabilization of wine and other vegetable drinks and related stabilization process" University of Bologna, granted 05/2020; International patent application: PCT/IB2019/053102, 2018. The other authors declare no conflicts of interest.

Data Availability Statement

The data that support the findings of this study are available on request from the corresponding author. The data are not publicly available due to privacy or ethical restrictions.

References

1. E. J. Waters, N. J. Shirley, and P. J. Williams, "Nuisance Proteins of Wine Are Grape Pathogenesis-Related Proteins," *Journal of Agricultural and Food Chemistry* 44, no. 1 (1996): 3–5, https://doi.org/10.1021/jf9505584.

2. K. F. Pocock, Y. Hayasaka, M. G. McCarthy, and E. J. Waters, "Thaumatin-Like Proteins and Chitinases, The Haze-Forming Proteins of Wine, Accumulate During Ripening of Grape (*Vitis vinifera*) Berries and Drought Stress Does Not Affect the Final Levels per Berry at Maturity," *Journal of Agricultural and Food Chemistry* 48, no. 5 (2000): 1637–1643, https://doi.org/10.1021/jf9905626.

3. M. Marangon, S. C. V. Sluyter, P. A. Haynes, and E. J. Waters, "Grape and Wine Proteins: Their Fractionation by Hydrophobic Interaction Chromatography and Identification by Chromatographic and Proteomic Analysis," *Journal of Agricultural and Food Chemistry* 57, no. 10 (2009): 4415–4425, https://doi.org/10.1021/jf9000742.

4. M. Marangon, S. C. Van Sluyter, E. J. Waters, and R. I. Menz, "Structure of Haze Forming Proteins in White Wines: *Vitis vinifera* Thaumatin-Like Proteins," *PLoS One* 9, no. 12 (2014): 1–21, https://doi.org/10.1371/journal.pone.0113757.

5. S. Vincenzi, M. Marangon, S. Tolin, and A. Curioni, "Protein Evolution During the Early Stages of White Winemaking and Its Relations With Wine Stability," *Australian Journal of Grape and Wine Research* 17, no. 1 (2011): 20–27, https://doi.org/10.1111/j.1755-0238.2010.00113.x.

6. F. Cosme, C. Fernandes, T. Ribeiro, L. Filipe-Ribeiro, and F. M. Nunes, "White Wine Protein Instability: Mechanism, Quality Control and

Technological Alternatives for Wine Stabilisation: An Overview," *Beverages* 6 (2020): 1–28, https://doi.org/10.3390/beverages6010019.

7. I. Horvat, S. Radeka, T. Plavša, and I. Lukić, "Bentonite Fining During Fermentation Reduces the Dosage Required and Exhibits Significant Side-Effects on Phenols, Free and Bound Aromas, and Sensory Quality of White Wine," *Food Chemistry* 285 (2019): 305–315, https://doi.org/10.1016/j.foodchem.2019.01.172.

8. S. Sommer, S. J. Sommer, and M. Gutierrez, "Characterization of Different Bentonites and Their Properties as a Protein-Fining Agent in Wine," *Beverages* 8, no. 2 (2022): 31, https://doi.org/10.3390/beverages8020031.

9. A. Mierczynska-Vasilev, P. Boyer, K. Vasilev, and P. A. Smith, "A Novel Technology for the Rapid, Selective, Magnetic Removal of Pathogenesis-Related Proteins From Wines," *Food Chemistry* 232 (2017): 508–514, https://doi.org/10.1016/j.foodchem.2017.04.050.

10. A. Mierczynska-Vasilev, S. K. Wahono, P. A. Smith, K. Bindon, and K. Vasilev, "Using Zeolites to Protein Stabilize White Wines," *ACS Sustainable Chemistry & Engineering* 7 (2019): 12240–12247.

11. T. Abbot and E. Wilkes, "Further Understanding of Bentonite's Impact on Metals in Wine," *Australian Wine Research Institute* (2018): 11–15.

12. S. Bheemathati, "Nanotechnology in Oenology," *Journal of Food Processing & Beverages* 6 (2018): 1–4.

13. G.-D. Dumitriu, N. L. de Lerma, V. V. Cotea, and R. A. Peinado, "Application of Mesoporous Materials as Fining Agents for Pedro Ximénez Wines," *Advances in Food Science and Engineering* 2, no. 1 (2018): 23–29, https://doi.org/10.22606/afse.2018.21003.

14. D. Silva-Barbieri, F. N. Salazar, F. López, N. Brossard, N. Escalona, and J. R. Pérez-Correa, "Advances in White Wine Protein Stabilization Technologies," *Molecules* 27, no. 4 (2022): 1251, https://doi.org/10.3390/molecules27041251.

15. D. Silva-Barbieri, N. Escalona, F. N. Salazar, F. López, and J. R. Pérez-Correa, "Novel Protein Stabilization in White Wine: A Study on Thermally Treated Zirconia-Alumina Composites," *Food Research International* 186 (2024): 114337, https://doi.org/10.1016/j.foodres.2024.114337.

16. I. Garmendia Aguirre, E. Abbate, G. Bracalente, et al., "Safe and Sustainable by Design Chemicals and Materials," *Revised Framework* (Publications Office of the European Union, 2025).

17. R. Ahmad and M. Sardar, "Enzyme Immobilization: An Overview on Nanoparticles as Immobilization Matrix," *Biochemistry & Analytical Biochemistry* 04 (2015): 1–8.

18. S. Liu, X. Y. Meng, J. M. Perez-Aguilar, and R. Zhou, "An in Silico Study of TiO2 Nanoparticles Interaction With Twenty Standard Amino Acids in Aqueous Solution," *Scientific Reports* 6 (2016): 1–10, https://doi.org/10.1038/srep37761.

19. T. Degabriel, C. Dupont-gillain, and J. Lambert, *Study of the interaction between proteins and TiO2 NPs: nature of the interfacial processes, PhD Thesis* (Pierre and Marie Curie University, 2017).

20. K. I. Omoniyi, "Adsorption of the Proteins of White Wine Onto Activated Carbon, Alumina and Titanium Dioxide," *African Journal of Pure and Applied Chemistry* 3 (2009): 6–10.

21. A. Sachko, I. Kobasa, O. Moysyura, and Y. Fedkovych, "Perspective of Utilization of Nanodispersive Materials Based on SiO2, TiO2 and SiO2-TiO2 for Wine Fining," *Journal of Food Process Engineering* 16 (2018): 216–221.

22. G. P. Parpinello, A. Ricci, M. Serantoni, A. Balducci, L. Ragni, and A. Versari, "A New Device for Stabilization of White Wines Throughout a Continuous Flow System," *Internet Journal of Viticulture and Enology* no. 1/1 (2020).

23. C. Baldisserri, S. Ortelli, M. Blosi, and A. L. Costa, "Pilot-Plant Study for the Photocatalytic/Electrochemical Degradation of Rhodamine B," *Journal of Environmental Chemical Engineering* 6, no. 2 (2018): 1794–-1804, https://doi.org/10.1016/j.jece.2018.02.008.

24. D. L. Cunha, A. Kuznetsov, C. A. Achete, A. E. D. H. Machado, and M. Marques, "Immobilized TiO2 on Glass Spheres Applied to Heterogeneous Photocatalysis: Photoactivity, Leaching and Regeneration Process," *PeerJ* 6 (2018): 1–19, https://doi.org/10.7717/peerj.4464.

25. I. Levchuk and M. Sillanpää, "Titanium Dioxide–Based Nanomaterials for Photocatalytic Water Treatment," *Advanced Water Treatment* 1 (2020): 1–56.

26. L. Faccani, S. Ortelli, M. Blosi, and A. L. Costa, "Ceramized Fabrics and Their Integration in a Semi-Pilot Plant for the Photodegradation of Water Pollutants," *Catalysts* 11 (2021): 1418, https://doi.org/10.3390/catal11111418.

27. L. R. Paez and J. Matoušek, "Properties of Sol-Gel TiO2 Layers on Glass Substrate," *Ceramics-Silikáty* 48 (2004): 66–71.

28. A. El Yadini, H. Saufi, P. S. M. Dunlop, J. A. Byrne, M. E. Azzouzi, and S. E. Hajjaji, "Supported TiO2 on Borosilicate Glass Plates for Efficient Photocatalytic Degradation of Fenamiphos," *Journal of Catalysis* 2014 (2014): 1–8, https://doi.org/10.1155/2014/413693.

29. I. Truijen, I. Haeldermans, M. K. Van Bael, et al., "Influence of Synthesis Parameters on Morphology and Phase Composition of Porous Titania Layers Prepared via Water Based Chemical Solution Deposition," *Journal of the European Ceramic Society* 27, no. 16 (2007): 4537–4546, https://doi.org/10.1016/j.jeurceramsoc.2007.02.200.

30. M. Taylor, R. C. Pullar, I. P. Parkin, and C. Piccirillo, "Nanostructured Titanium Dioxide Coatings Prepared by Aerosol Assisted Chemical Vapour Deposition (AACVD)," *Journal of Photochemistry and Photobiology A: Chemistry* 400 (2020): 112727, https://doi.org/10.1016/j.jphotochem.2020.112727.

31. A. Ricci, A. Versari, L. Ragni, and G. P. Parpinello, "Effect of an Innovative Sorbent Material Coupled to Continuous Flow Process in the Protein and Oxidative Stability of White Wines," *Food Chemistry* 446 (2024): 138868, https://doi.org/10.1016/j.foodchem.2024.138868.

32. G. P. Parpinello, A. Versari, L. Ragni, A. Ricci, M. Serantoni, and A. Balducci, "Patent No. 102018000004721-Device for the Stabilization of Wine and Other Vegetable Drinks and Related Stabilization Process" (2018).

33. M. R. Sarmento, J. C. Oliveira, and R. B. Boulton, "Selection of Low Swelling Materials for Protein Adsorption From White Wines," *International Journal of Food Science and Technology* 35, no. 1 (2000): 41–47, https://doi.org/10.1046/j.1365-2621.2000.00340.x.

34. S. Vincenzi, S. Mosconi, G. Zoccatelli, et al., "Development of a New Procedure for Protein Recovery and Quantification in Wine," *American Journal of Enology and Viticulture* 56, no. 2 (2005): 182–187, https://doi.org/10.5344/ajev.2005.56.2.182.

35. A. Mierczynska-Vasilev, K. Bindon, R. Gawel, et al., "Fluorescence Correlation Spectroscopy to Unravel the Interactions Between Macromolecules in Wine," *Food Chemistry* 352 (2021): 129343, https://doi.org/10.1016/j.foodchem.2021.129343.

36. A. Lolli, M. Blosi, S. Ortelli, et al., "Innovative Synthesis of Nanostructured Composite Materials by a Spray-Freeze Drying Process: Efficient Catalysts and Photocatalysts Preparation," *Catalysis Today* 334 (2019): 193–202, https://doi.org/10.1016/j.cattod.2018.11.022.

37. S. Ortelli, A. L. Costa, I. Zanoni, et al., "TiO2@BSA Nano-Composites Investigated Through Orthogonal Multi-Techniques Characterization Platform," *Colloids Surfaces B Biointerfaces* 207 (2021): 112037, https://doi.org/10.1016/j.colsurfb.2021.112037.

38. K. F. Pocock and B. C. Rankine, "Heat Test for Detecting Protein Instability in Wine," *Australian Wine, Brewing and Spirit Review* 91 (1973): 42–43.

39. E. J. Waters, G. Alexander, R. Muhlack, et al., "Preventing Protein Haze in Bottled White Wine," *Australian Journal of Grape and Wine*

Research 11, no. 2 (2005): 215–225, https://doi.org/10.1111/j.1755-0238.2005.tb00289.x.

40. S. C. Van Sluyter, J. M. McRae, R. J. Falconer, et al., "Wine Protein Haze: Mechanisms of Formation and Advances in Prevention," *Journal of Agricultural and Food Chemistry* 63, no. 16 (2015): 4020–4030, https://doi.org/10.1021/acs.jafc.5b00047.

41. V. Moine-Ledoux and D. Dubourdieu, "An Invertase Fragment Responsible for Improving the Protein Stability of Dry White Wines," *Journal of the Science of Food and Agriculture* 79, no. 4 (1999): 537–543, https://doi.org/10.1002/(sici)1097-0010(19990315)79:4%3C537::aid-jsfa214%3E3.3.co;2-2.

42. J. W. Bye, S. Meliga, D. Ferachou, G. Cinque, J. A. Zeitler, and R. J. Falconer, "Analysis of the Hydration Water Around Bovine Serum Albumin Using Terahertz Coherent Synchrotron Radiation" (2014).

43. K. Shimada and S. Matsushita, "Thermal Coagulation of Bovine Serum Albumin," *Agricultural and Biological Chemistry* 45, no. 9 (1981): 1945–1952, https://doi.org/10.1080/00021369.1981.10864826.

44. A. Tsutomu and S. N. Timasheff, "Mechanism of Protein Salting in and Salting Out by Divalent Cation Salts: Balance Between Hydration and Salt Binding," *Biochemistry* 23 (1984): 5912–5923.

45. P. K. Smith, R. I. Krohn, G. T. Hermanson, et al., "Measurement of Protein Using Bicinchoninic Acid," *Analytical Biochemistry* 150, no. 1 (1985): 76–85, https://doi.org/10.1016/0003-2697(85)90442-7.

46. N. Miranda-García, S. Suárez, M. I. Maldonado, S. Malato, and B. Sánchez, "Regeneration Approaches for TiO2 Immobilized Photocatalyst Used in the Elimination of Emerging Contaminants in Water," *Catalysis Today* 230 (2014): 27–34, https://doi.org/10.1016/j.cattod.2013.12.048.

47. S. Ortelli, A. L. Costa, and M. Dondi, "TiO2 Nanosols Applied Directly on Textiles Using Different Purification Treatments," *Materials* 8, no. 11 (2015): 7988–7996, https://doi.org/10.3390/ma8115437.

48. F. Borghi, V. Vyas, A. Podestà, and P. Milani, "Nanoscale Roughness and Morphology Affect the Isoelectric Point of Titania Surfaces," *PLoS One* 8, no. 7 (2013): 1–14, https://doi.org/10.1371/journal.pone.0068655.

49. C. E. Giacomelli, M. J. Avena, and C. P. De Pauli, "Adsorption of Bovine Serum Albumin Onto TiO2 Particles," *Journal of Colloid and Interface Science* 188, no. 2 (1997): 387–395, https://doi.org/10.1006/jcis.1996.4750.

50. F. Y. Oliva, L. B. Avalle, O. R. Cámara, and C. P. De Pauli, "Adsorption of Human Serum Albumin (HSA) Onto Colloidal TiO2 Particles, Part I," *Journal of Colloid and Interface Science* 261, no. 2 (2003): 299–311, https://doi.org/10.1016/s0021-9797(03)00029-8.

51. J. Płotka-Wasylka, M. Frankowski, V. Simeonov, Ż. Polkowska, and J. Namieśnik, "Determination of Metals Content in Wine Samples by Inductively Coupled Plasma-Mass Spectrometry," *Molecules* 23 (2018): 1–11, https://doi.org/10.3390/molecules23112886.

52. M. Younes, G. Aquilina, L. Castle, et al., "Safety Assessment of Titanium Dioxide (E171) as a Food Additive," *EFSA Journal* 19, no. 5 (2021): https://doi.org/10.2903/j.efsa.2021.6585.

53. M. C. F. Karlsson, R. Álvarez-Asencio, R. Bordes, A. Larsson, P. Taylor, and B. M. Steenari, "Characterization of Paint Formulated Using Secondary TiO2 Pigments Recovered From Waste Paint," *Journal of Coatings Technology and Research* 16 (2019): 607–614, https://doi.org/10.1007/s11998-018-0132-x.

54. DAFNE-Departmentof Agronomy Food Natural resources Animals and Environment, *Project Vinosme* (Padova Univeristy, 2009), https://www.dafnae.unipd.it/ricerca/progetti-di-ricerca/progetti-conclusi/progetto-vinosme.

Supporting Information

Additional supporting information can be found online in the Supporting Information section. *(Supporting Information)*

Table S1 Chemical composition of 5-mm-diameter glass spheres used as an inert support for the adsorbing thin layers.

Table S2 Data on Rosé wine (vintage 2021).

Table S3 Glass sphere surface treatment and TiO_2 and TiO_2@SiO_2 nanosol coating.

Table S4 Cu and Fe ions in Rosé wine measured by ICP–OES.

Figure S1 Regeneration of spheres after use: on the left, spheres immediately after contact with wine, in the centre spheres immersed in the NaOH solution, at the bottom the beaker containing the spilt solution of NaOH and the proteins detached from the spheres, on the right, spheres after washing with water until neutral reaction.

Figure S2 FE-SEM images of glass sphere surface: a) as received; b) sandblasted surface.

Figure S3 FE-SEM images of TiO_2 nanosol-coated spheres: a) TQ–TiO_2, b) TQ–TiO_2@SiO_2, c) TA–TiO_2, d) TA–TiO_2@SiO_2, e) TB–TiO_2, f) TB–TiO_2@SiO_2 thin layers on sphere surface.

Figure S4 Turbidimetry values (NTUm) measured for the two types of TiO_2 nanosol-coated material, a) TiO_2 and b) TiO_2@SiO_2-coated samples, in the 3 washing cycles, for a total of 25, 50 and 75 mL of used water.

Figure S5 ICP–OES measurement of TiO_2 release in the washing water, from nanosol-coated spheres, after 3 washing cycles; ∗value < LOD.

Figure S6a BSA determination by the HTP–BSA method: BSA calibration curve (blue dots); BSA content after contact with the coated spheres: yellow dots: TiO_2 nanosol (BSA range 102–107 mg/L); red dots: TiO_2@SiO_2 nanosol (BSA range 121–129 mg/L); green dot: TiO_2 paste coated (BSA 91 mg/L).

Figure S6b BSA determination by ICP–OES analysis: BSA calibration curve (blue dots); BSA content after contact with the coated spheres: yellow dots: TiO_2 nanosol; red dots: TiO_2@SiO_2 nanosol.

Figure S6c BSA determination by UV–Vis analysis: BSA calibration curve (blue dots); BSA content after contact with the TiO_2 nanosol-coated spheres: orange dots.

Figure S7 Comparison of the methods used for assessing the content of BSA (mg/L) of TiO_2 nanosol-coated spheres.

Figure S8 Adsorption capability of the TiO_2 paste-coated spheres during 8 regeneration cycles: a) expressed as a percentage of BSA adsorbed, b) normalised adsorption values.

Figure S9 TiO_2 release during regeneration cycles after adsorption from the model wine solution. An ICP–OES analysis of the TiO_2 content in the treated model wine solution indicated a TiO_2 release decreasing from 0.5 mg/L to 0.04 mg/L after the sixth cycle.

Supplementary figure and table legend

Table S1 Chemical composition of 5 mm diameter glass spheres used as an inert support for the adsorbing thin layers.

Chemical composition % w/w					
SiO_2	61 - 67	CaO	5 - 10	Na_2O	10 - 18
Al_2O_3	3 - 8	MgO	0.5 – 3.0	B_2O_3	1 - 5
Lead-free					

Table S2 Data on Rosé wine (vintage 2021).

Bentonite demand	**1 g/L**
Picking time	10 October 2021
Must density	1084 = 84°Oe
Acidity	7.5 g/L
pH	3.1
Added of SO_2 3_11_2021	70 mg/L

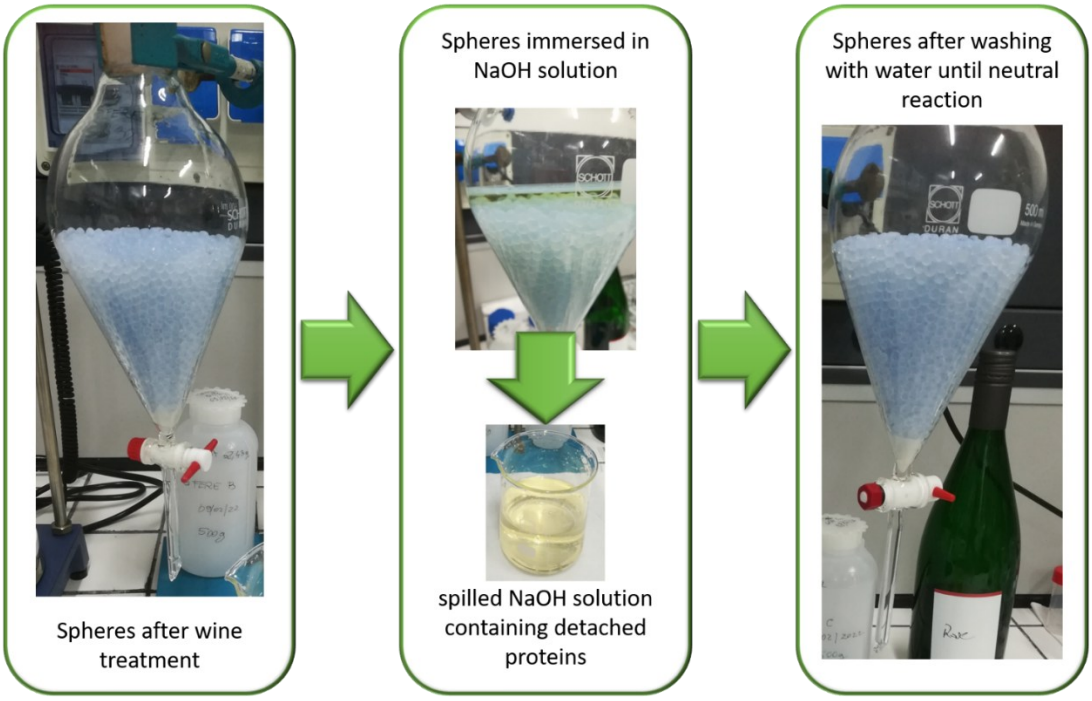

Figure S1 Regeneration of spheres after use: on the left, spheres immediately after contact with wine, in the centre spheres immersed in the NaOH solution, at the bottom the beaker containing the spilt solution of NaOH and the proteins detached from the spheres, on the right, spheres after washing with water until neutral reaction.

Table S3 Glass spheres surface treatment and TiO_2 and TiO_2@SiO_2 nanosol coating.

Spheres type	nanosol TiO_2	nanosol TiO_2@SiO_2
Untreated surface (TQ)	x	x
Acidic treatment (TA)	x	x
Basic treatment (TB)	x	x

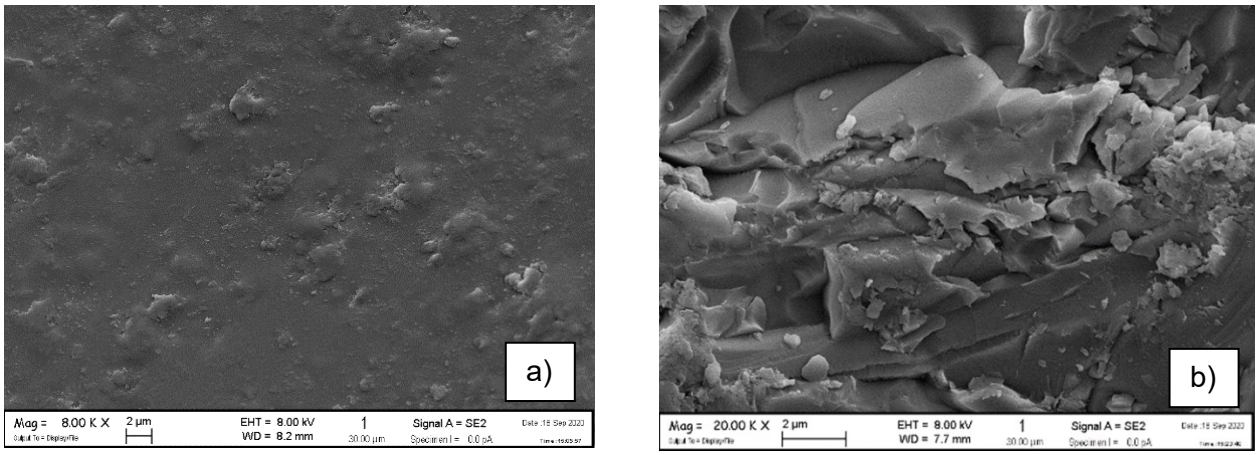

Figure S2 FESEM images of glass spheres surface: a) as received; b) sandblasted surface.

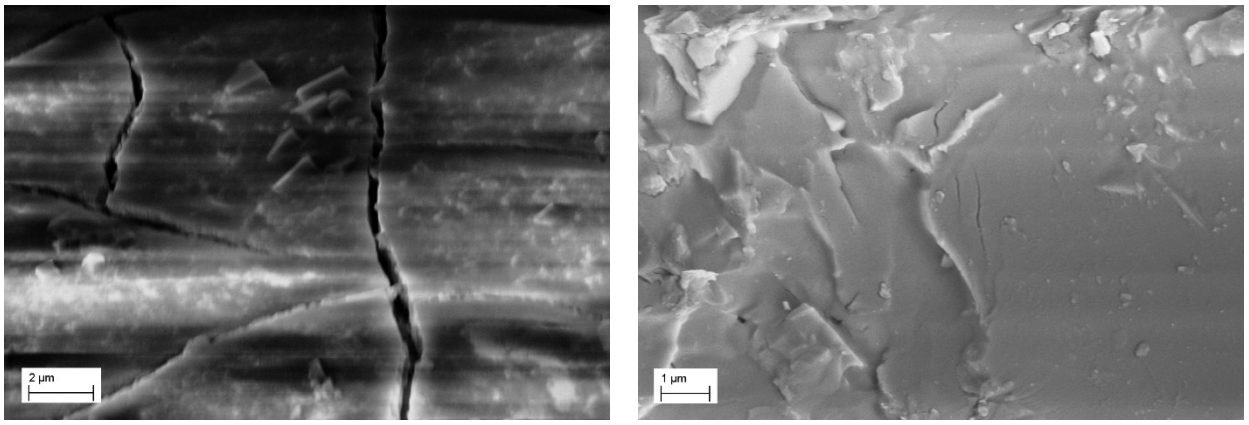

a) TQ - TiO_2 *b) TQ - TiO_2@SiO_2*

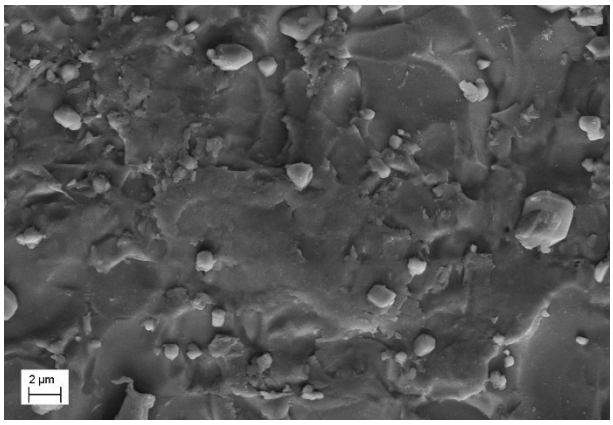

c) TA - TiO_2

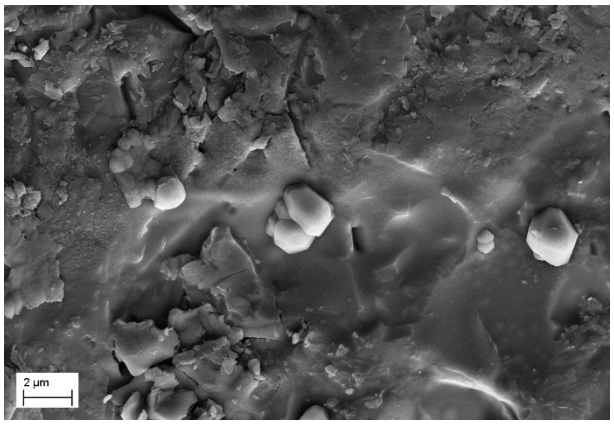

d) TA - TiO_2@SiO_2

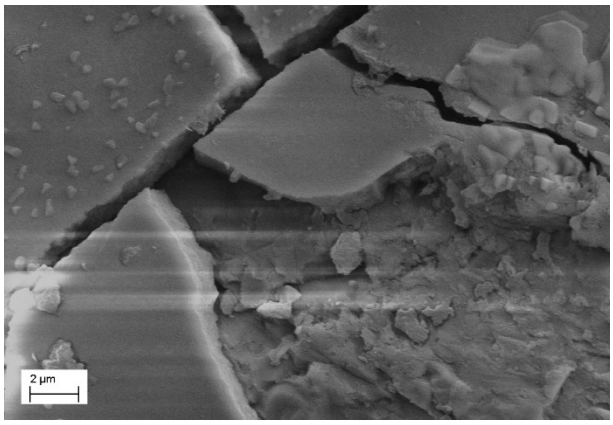

e) TB - TiO_2

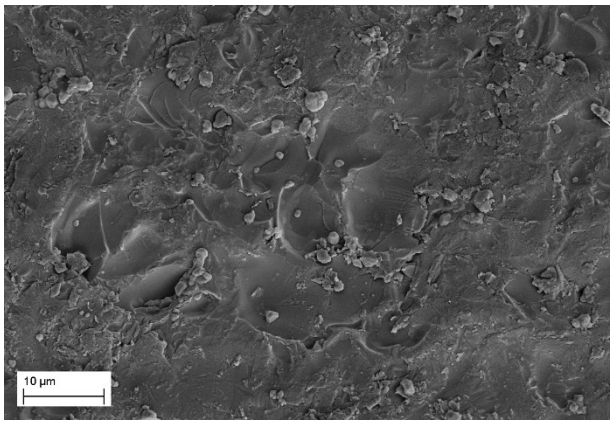

f) TB - TiO_2@SiO_2

Figure S3 FESEM images of TiO2 nanosol-coated spheres: a) ***TQ - TiO_2****, b)* ***TQ - TiO_2@SiO_2****, c)* ***TA - TiO_2****, d)* ***TA - TiO_2@SiO_2****, e)* ***TB - TiO_2****, f)* ***TB - TiO_2@SiO_2*** *thin layers on spheres surface.*

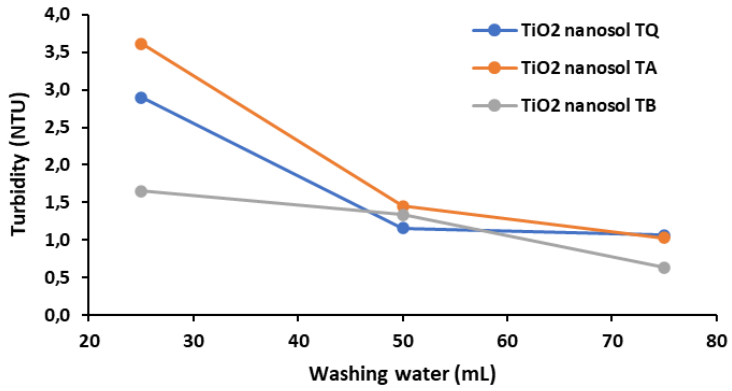

a)

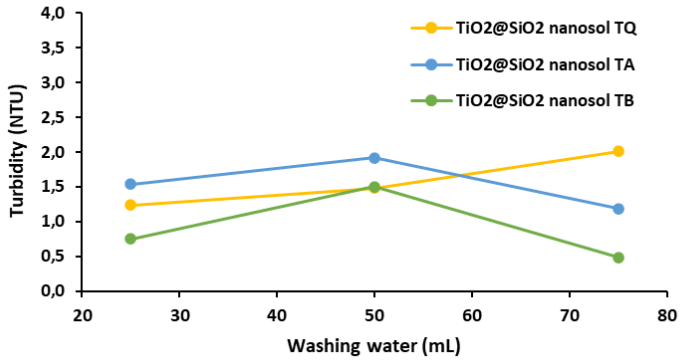

b)

Figure S4 Turbidimetry values (NTUm) measured for the two types of TiO_2 nanosol-coated material, a) TiO_2 and b) TiO_2@SiO_2 coated samples, in the 3 washing cycles, for a total of 25, 50, and 75 mL of used water.

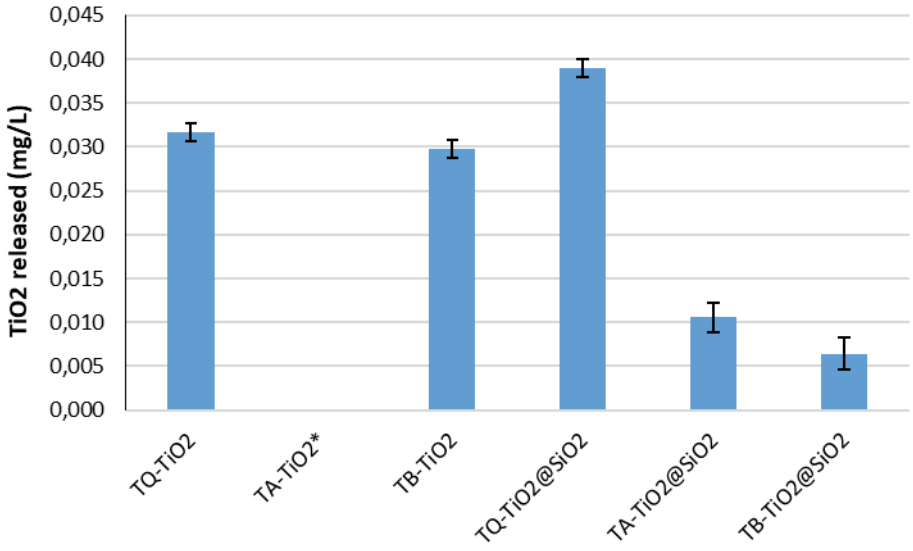

*Figure S5 ICP-OES measurement of TiO_2 release in the washing water, from nanosol-coated spheres, after 3 washing cycles; *value < LOD*

BSA detection in model wine solutions: HTP-BSA, ICP-OES and UV-Vis analysis

To determine if the HTS-BSA method was appropriate to measure the BSA adsorption from the model wine solutions by the TiO_2 nanosol-coated spheres treatment, we compared three methods: the HTP-BSA (Figure S6a), the ICP-OES (Figure S6b) and a UV-Vis analysis (Figure S6c) to detect the BSA absorbance at 280 nm. Figure S7 compares the BSA content measured in the six solutions after contact with the new adsorbing materials by the three techniques. It is possible to see that BSA content measured by HTP-BSA and by ICP-OES analysis have a similar trend, indicating that the TiO_2 nanosol-coating is more efficient than the TiO_2@SiO_2 nanosol. The error bar in the ICP-OES is high, due to the alcoholic content of the model wine solution that required a multi-step dilution. The BSA concentrations obtained by UV-Vis analysis resulted in an overestimation: 160 mg/L of BSA vs 140 mg/L (nominal concentration), which resulted therefore affected by a systematic error caused

by the TiO_2 leakage in the solution, and an overlapping of the TiO_2 adsorption spectra at 278-280 nm to the adsorption peak of the BSA (280 nm), affecting the reading of the results. Because of this, the HTP-BSA method results, in this case, a more sensitive and direct method to measure the BSA content in the model wine solutions.

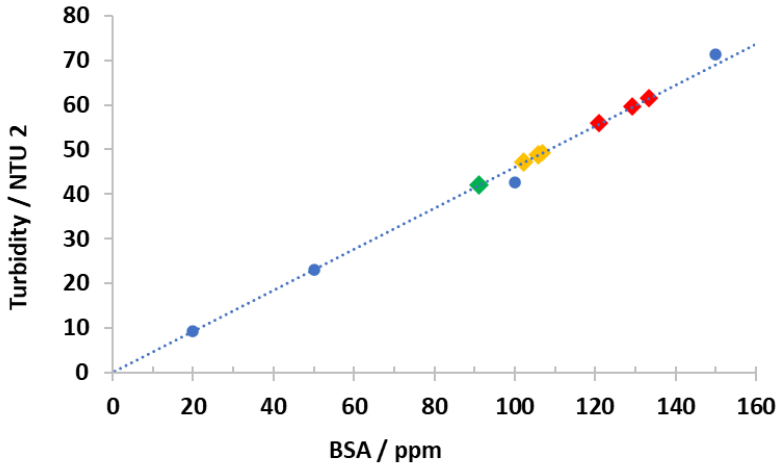

Figure S6a BSA determination by HTP-BSA method: BSA calibration curve (blue dots); BSA content after contact with the coated spheres: yellow dots: TiO_2 nanosol (BSA range 102-107 mg/L); red dots: TiO_2@SiO_2 nanosol (BSA range 121-129 mg/L); green dot: TiO_2 paste coated (BSA 91 mg/L)

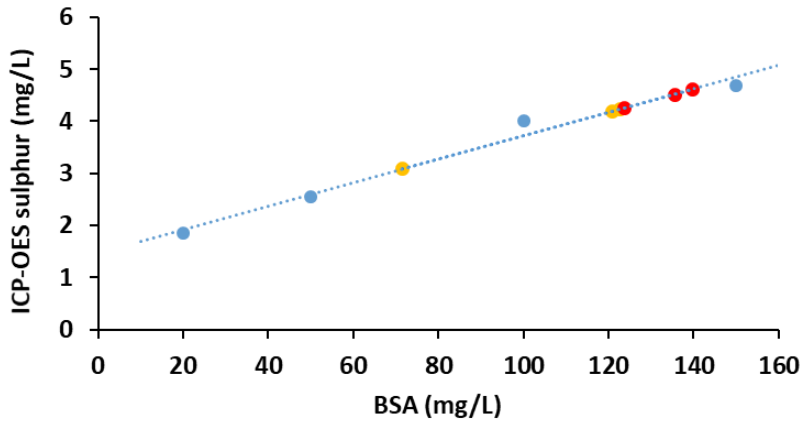

Figure S6b BSA determination by ICP-OES analysis: BSA calibration curve (blue dots); BSA content after contact with the coated *spheres*: *yellow dots: TiO_2 nanosol; red dots: TiO_2@SiO_2 nanosol.*

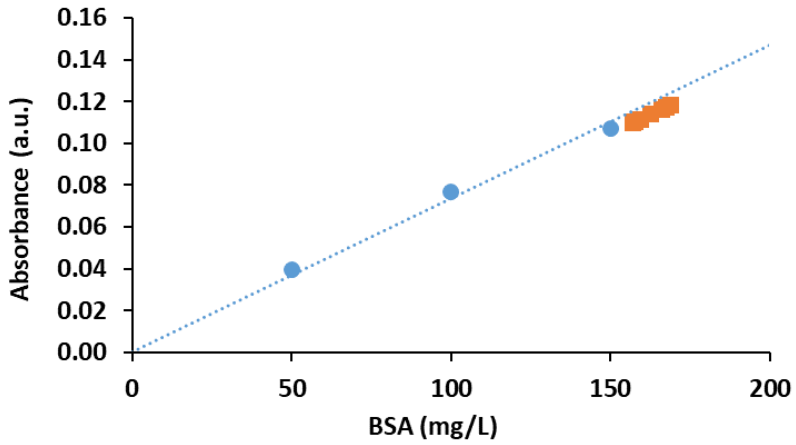

Figure S6c BSA determination by UV-Vis analysis: BSA calibration curve (blue dots); BSA content after contact with the TiO_2 nanosol-coated spheres: orange dots.

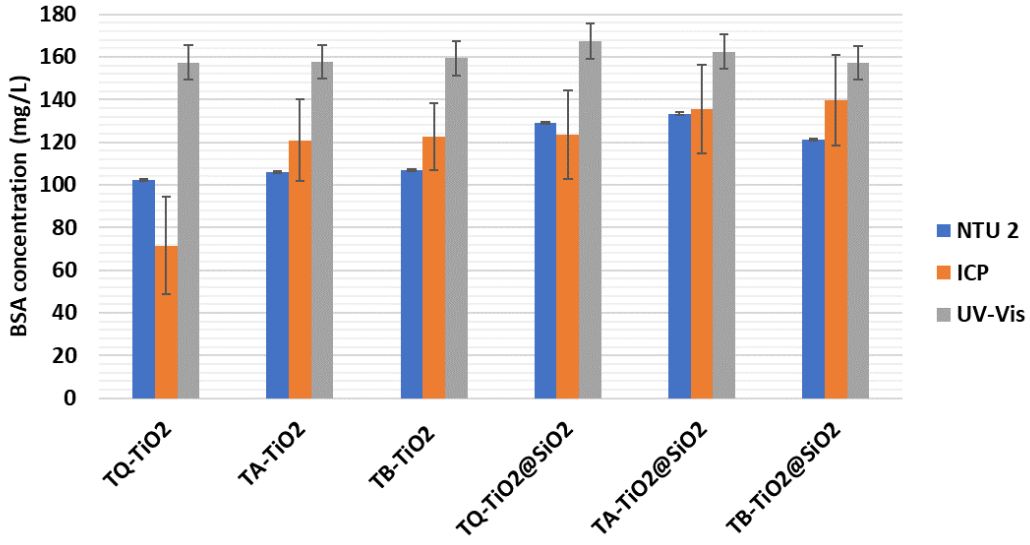

Figure S7 Comparison of the methods used for assessing the content of BSA (mg/L) of TiO_2 nanosol-coated spheres.

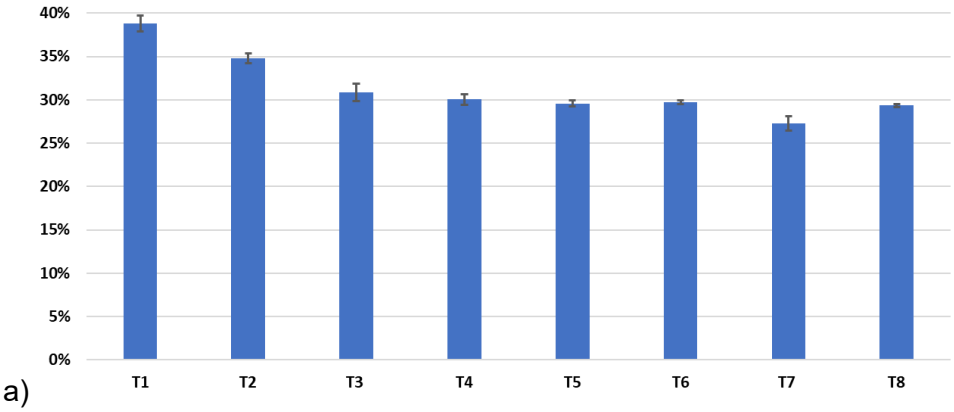

a)

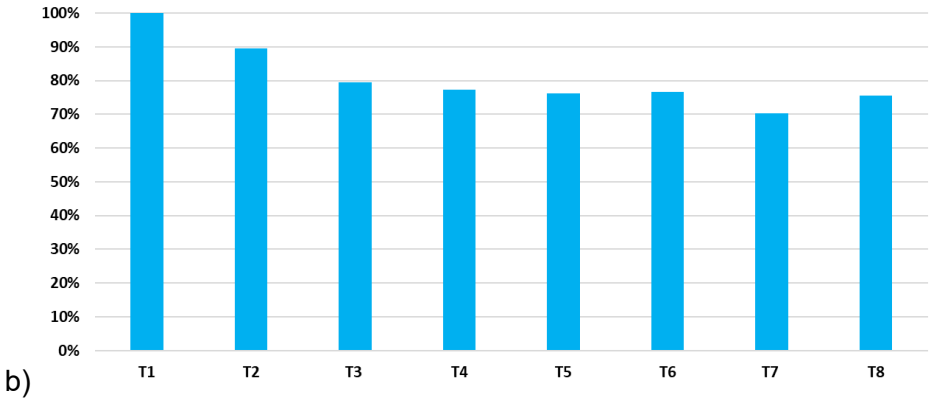

b)

Figure S8 Adsorption capability of the TiO_2 paste-coated spheres during 8 regeneration cycles a) expressed as a percentage of BSA adsorbed, b) normalized adsorption values.

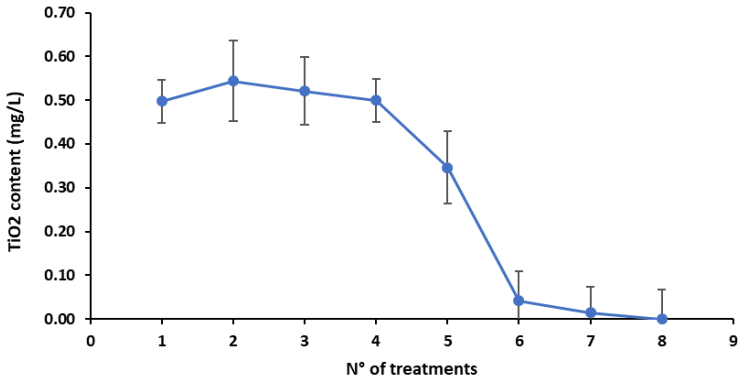

Figure S9 TiO_2 release during regeneration cycles after adsorption from the model wine solution. An ICP-OES analysis of the TiO_2 content in the treated model wine solution indicated a TiO_2 release decreasing from 0.5 mg/L to 0.04 mg/L after the 6th cycle.

Table S4 Cu and Fe ions in Rosé wine measured by ICP-OES.

	Cu (mg/L)	**Fe (mg/L)**	**TiO_2 (mg/L)**
Rosé wine untreated	1.40 ± 0.10	1.20 ± 0.07	Low*
Rosé wine treated	0.12 ± 0.04	1.1± 0.1	0.5 ± 0.01

* < LOD (0.01 mg/L)